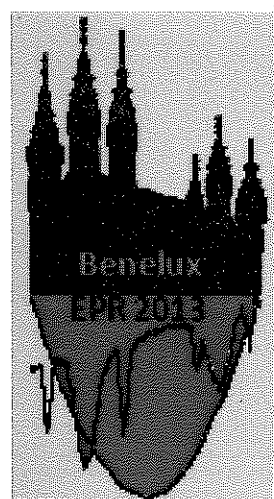


21st Benelux EPR meeting

Programme and Abstracts



University of Leuven
Semiconductor Physics Laboratory
Department of Physics and Astronomy

Campus Library Arenberg
3001 Leuven-Heverlee, Belgium

23 May 2013

Organization

Andre Stesmans
Semiconductor Physics Laboratory
Department of Physics and Astronomy
Celestijnenlaan 200 D
3001 Leuven, Belgium

21st Meeting of the Benelux EPR Group University of Leuven – May 23, 2013

- 9.45 *Registration + poster display + coffee/tea*
- 10.25 *Welcome*
- 10.30 **Multifrequency CW EPR, Pulse EPR and DFT Study of Solutions of** O1
 11.01 **Ti(III) Chloride in Various Organic Bases**
 Sara Maurelli^{1,2,*}, Mario Chiesa², Sabine Van Doorslaer¹
¹*Spectroscopy in Biophysics and Catalysis Group, Department of Physics, University of Antwerp, Belgium;* ²*Dipartimento di Chimica, Università di Torino, Italy;* **Dutch Polymer Institute (DPI), the Netherlands*
- 10.55 **Induction of mild hypothermia to target exacerbated metabolism of cancer** O2
cells : effect on energy producing pathways and intratumoral oxygenation.
 G. De Preter^a, C. De Riemaeker^a, P. Porporato^b, B. Jordan^a, P. Sonveaux^b and B. Gallez^a
^a*Biomedical Magnetic Resonance Unit,* ^b*Unit of Pharmacology & Therapeutics, Université Catholique de Louvain, Brussels, Belgium.*
- 11.20 **Detection of mitochondrial ROS formation by EPR in cultured cells and** O3
mice indicating mitochondrial dysfunctioning in toxicity and disease
 Jacob-Jan (Jacco) Briedé, Jian Jiang, Theo M.C.M. de Kok, Jos C.S. Kleinjans
Department of Toxicogenomics, Faculty of Health, Medicine and Life Sciences (FHML), School for Oncology and Developmental Biology (GROW), Maastricht University, Maastricht, the Netherlands
- 11.45 **EPR studies of endogenous radicals in human skin.** O4
 E. van Faassen¹ and C Suschek²
¹*Dept. of Nephrology, Leiden University Medical Centre, Leiden, the Netherlands*
²*Dept. of Trauma and hand surgery, Heinrich Heine University Hospital, Düsseldorf – FRG*
- 12.10 *Lunch and group picture*
- 14.00 **Effects of synthesis conditions on properties of ethane-bridged periodic** O5
mesoporous materials as revealed by spin-probe EPR
 Feng Lin,^{a,b} Pegie Cool,^b Sabine Van Doorslaer,^a
^a*Department of Physics, University of Antwerp, Antwerp, (Belgium).*
^b*Department of Chemistry, University of Antwerp, Antwerp, (Belgium).*
- 14.25 **Nitroxide spin labels for in-cell EPR** O6
 Mykhailo Azarkh
Department of Molecular Physics, Leiden University, Leiden, the Netherlands
- 14.50 **Single-crystalline arrays of thermally oxidized Si nanowires studied by** O7
electron spin resonance: the influence of nanowire diameter
 M. Jivănescu¹, A. Stesmans¹, and R. Kurstjens²
¹*Department of Physics and Astronomy, University of Leuven, Celestijnenlaan 200 D, 3001 Leuven, Belgium.* ²*IMEC, Kapeldreef 75, 3001 Leuven, Belgium*

15.15 *Coffee break — poster session*

15.45 **The type 1 copper site of pseudoazurin** O8
Edgar J.J. Groenen, Freek Broeren, Peter Gast, Takamitsu Kohzuma, and Silvia Sottini
Molecular Nano-Optics and Spins, Huygens Laboratory, Leiden University, Leiden, the Netherlands

16.10 *General discussion and closing remarks*

16.30 *Poster session + Reception*

18.30 *End*

Poster presentations

- Formation of Nitrosylated Hemoglobin in Human Venous Blood as Surrogate Index of Vascular Endothelial Function.** P1
I. Lobysheva¹, P. Biller¹, F. Dei Zotti¹, B. Gallez³, C. Beauloye², J.L. Balligand¹
(1) Pole of Pharmacology and Therapeutics, (2) Pole of Cardiovascular Pathology, Institute de Recherche Experimentale et Clinique, and (3) Magnetic Resonance Unit, Louvain Drug Research Institute, Université Catholique de Louvain, Brussels, Belgium
- Optically detected magnetic resonance study of NV⁻ centers in diamond** P2
Boris Yavkin, Shashi Singham, Etienne Govaerts
Department of Physics, University of Antwerp, Antwerp, Belgium.
- Q-band EMR study of radicals in X-irradiated L-threonine** P3
Gauthier Vanhaelewyn, Henk Vrielinck and Freddy Callens
Department of Solid State Sciences, Ghent University, Krijgslaan 281 - S1, 9000 Gent, Belgium
- Inherent interface defects at the thermal (211)Si/SiO₂ interface** P4
S. Iacovo ad A. Stesmans
Semiconductor Physics Laboratory, Department of Physics and Astronomy, University of Leuven, Celestijnenlaan 200 D, B-3001 Leuven, Belgium
- ODMR study of formation of triplet state in PCBM via photoinduced charge transfer in Super Yellow PPV: PCBM blend films** P5
Biniam Zerai Tedlla¹, Zhu Feng², Janssen Paul², Bert Koopmans², Etienne Goovaerts¹
¹*Department of Physics, University of Antwerp, Universiteitsplein1, B-2610, Wilrijk, Antwerp, Belgium*
²*Physics of Nanostructures, Dept. of Applied Physics, Eindhoven University of Technology, P.O. Box 513, NL-5600 MB Eindhoven, The Netherlands*
- Comparison of human and icefish neuroglobin and cytoglobin** P6
B. Cuypers¹, W. Van Leuven², S. Vermeyle², S. Dewilde², and S. Van Doorslaer¹
¹*SIBAC Laboratory, Department of Physics, University of Antwerp*
²*PPES Laboratory, Department of Biomedical Sciences, University of Antwerp, Universiteitsplein 1, B-2610 Antwerp, Belgium*
- EPR study of point defects in thermal GaAs/GaAs-oxide structures** P7
S. Nguyen, V. V. Afanas'ev, and A. Stesmans
Semiconductor Physics Laboratory, Department of Physics, University of Leuven, 3001 Leuven, Belgium
- Electron paramagnetic resonance spectrometry and imaging in melanomas: A comparison between pigmented and nonpigmented human malignant melanomas.** P8
Quentin Godechal¹, Ghanem Ghanem², Martin Cook³, and Bernard Gallez¹
¹*Biomedical Magnetic Resonance, University of Louvain, Brussels, Belgium,*
²*Université libre de Bruxelles, Brussels, Belgium,*
³*Department of Histopathology, Royal Surrey County Hospital, Guildford, United Kingdom*

The large in vitro heterogeneity of chlorite dismutase of Magnetospirillum sp strain Lusitani P9

A. De Schutter¹, D. Freire², P. González², S. Van Doorslaer¹

¹ SIBAC laboratory, department of Physics, University of Antwerp, Belgium

² REQUIMTE, department of Chemistry, Faculty of Science and Technology, Universidade Lisboa Nova

ESR dating of Neogene marine sands from the southern North Sea basin, NE Belgium: first results P10

Beerten K.¹, Iacovo S.², Jivanescu M.², Stesmans A.², Vandenberghe N.³

¹ SCK-CEN, Institute Environment-Health-Safety, Mol, Belgium)

² Department of Physics, KULeuven, Leuven, Belgium

³ Department of Earth and Environmental Sciences, KULeuven, Leuven, Belgium

Influence of free radicals signal from dental resins on the radio-induced signal in teeth in nuclear retrospective dosimetry : kinetic analysis using electron paramagnetic resonance. P11

C. Desmet¹, Ph. Levêque¹, A. DosSantos², J. Leprince^{2,3}, G. Leloup^{2,3} and B. Gallez¹

¹ Biomedical Magnetic Resonance Group, Louvain Drug Research Institute, UCLouvain,

² School of Dental Medicine and Stomatology, UCLouvain

³ Centre de Recherche et d'Ingénierie en Biomatériaux CRIBIO, UCLouvain.

Electron spin resonance probing of defects in Si foils fabricated by the SLiM-Cut method. P12

J. Kepa¹, A. Stesmans¹, A. Masolin² and E. Simoen².

¹ Department of Physics and INPAC, University of Leuven, Celestijnenlaan 200 D, B-3001 Leuven, Belgium

² Imec, Kapeldreef 75, B-3001 Leuven, Belgium

Oral presentations

Multifrequency CW EPR, Pulse EPR and DFT Study of Solutions of Ti(III) Chloride in Various Organic Bases

Sara Maurelli^{1,2,*}, Mario Chiesa², Sabine Van Doorslaer¹

¹ Spectroscopy in Biophysics and Catalysis Group, Department of Physics, University of Antwerp, Belgium

² Dipartimento di Chimica, Università di Torino, Italy

* Dutch Polymer Institute (DPI), the Netherlands

X-band (9.7GHz) and W-band (94GHz) Continuous Wave (CW) and Pulse EPR methods have been applied to the study of Ti(III) chloride dissolved in different organic solvents. Hyperfine techniques (HYSCORE) in conjunction with DFT calculations are found to be a powerful method to elicit information on the type of nuclei surrounding the Ti^{3+} ion. For the first time, the hyperfine and nuclear quadrupole data of Ti(III)-bound Cl nuclei are reported. With the help of DFT models suggestions are made as to the structure of the observed species. Comparison is set to spectra recorded for the $[Ti(H_2O)_6]^{3+}$ reference system. The results are useful in understanding the nature of Ti(III) species in more complex systems such as $MgCl_2$ -supported Ti based High-Yield Ziegler-Natta Catalysts.

11:30

Induction of mild hypothermia to target exacerbated metabolism of cancer cells : effect on energy producing pathways and intratumoral oxygenation.

G. De Preter^a, C. De Riemaker^a, P. Porporato^b, B. Jordan^a, P. Sonveaux^b and B. Gallez^a
^a*Biomedical Magnetic Resonance Unit, ^bUnit of Pharmacology & Therapeutics, Université Catholique de Louvain, Brussels, Belgium.*

Most aggressive tumors are characterized by highly proliferative cells showing exacerbated metabolism. Angiogenesis, induced by tumor cells to sustain their growth, is chaotic with abnormal immature blood vessels, which leads to the emergence of hypoxic regions in tumors. Radio and chimio-resistance appearing in these areas is a major issue of cancer treatment, and strategies that relieve tumor hypoxia combined with current therapies are constantly developed and evaluated in clinical trials. Here, we propose to use mild hypothermia (32°C as commonly used in ICU) as a potent strategy to inhibit exacerbated cancer metabolism and to provide radiosensitizing properties. Metabolic alterations induced by mild hypothermia (32°C) were analysed on two different cancer cell lines: the human mammary cancer MDA-MB-231 exhibiting a Warburg phenotype (glycolytic) and the human uterine cancer SiHa exhibiting an oxidative phenotype. Oxygen consumption rate, reflecting mitochondrial respiration, was assessed using Electron Paramagnetic Resonance (EPR) oximetry with a neutral nitroxide as oxygen sensor. Glycolytic activity was assayed by glucose consumption and lactate production measurements from supernatants of cultured cells using enzymatic assays (CMA600). Intracellular ATP content was quantified using a commercially available kit. These experiments showed that mild hypothermia induced global hypometabolism in tumor cells, as shown by the respiration and the glycolytic activity slowdown accompanied by preserved ATP levels. In vivo, TLT tumor bearing mice were either cooled to 32°C (treated group) or kept at 37°C (control group) during 2 hours. Evolution of tumoral oxygenation was monitored using L-Band EPR with charcoal as oxygen sensor. Results showed a progressive improvement of oxygen level when mice were treated by mild hypothermia (2 fold increase in 2 hours) compared to the control group. The decrease in oxygen consumption rate of TLT cells observed *in vitro* could account for the reduction of tumor hypoxia observed *in vivo*. These findings are promising for a radiosensitizing effect of metabolism inhibition by mild hypothermia.

M:SS

Detection of mitochondrial ROS formation by EPR in cultured cells and mice indicating mitochondrial dysfunctioning in toxicity and disease

Jacob-Jan (Jacco) Briedé, Jian Jiang, Theo M.C.M. de Kok, Jos C.S. Kleinjans

Department of Toxicogenomics, Faculty of Health, Medicine and Life Sciences (FHML), School for Oncology and Developmental Biology (GROW), Maastricht University, Maastricht, The Netherlands

Increased formation of reactive oxygen species (ROS), including oxygen radicals like superoxide anion radicals, is one of the features of mitochondrial dysfunctioning that is thought to play a pivotal role in disease processes. Electron paramagnetic resonance (EPR) spectroscopy in combination with spin trapping technique is the only method available to directly identify and quantify changes in mitochondrial superoxide anion radical formation. This EPR approach was used in several studies to investigate the role of changes in ROS production by mitochondrial dysfunctioning as an important biomarker for ageing, toxicity and the onset of diseases.

For example, we analyzed changes in muscle mitochondrial ROS formation during aging as well as in a genetic mouse model overexpressing the mitochondrial uncoupling protein UCP3, hypothesized to play a role in diabetes. As expected, we detected increased muscle mitochondrial ROS production in 75 weeks old compared to 25 weeks old mice. Next to this we proved that UCP3 overexpressing mice showed decreased ROS formation.

We also investigated the effect of paracetamol (acetaminophen) in a liver cell line of hepatocytes (HepG2 cells). Mitochondrial dysfunction has been implicated as a major contributor to drug-induced toxicity (DILI) in the liver. Exposing HepG2 cells to a dose range of acetaminophen, isolating and subsequent detecting ROS formation by EPR spectroscopy showed a significant increase as indication for mitochondrial dysfunctioning. By analysing whole genome gene expression data (transcriptomics) we identified that mitochondrial-related processes as the electron transport chain and lipid and amino-acid metabolism are impaired, which could clarify the mechanism of acetaminophen-related liver toxicity.

Altogether, these studies showed that EPR spectroscopy is a valuable tool to investigate mechanisms of disease-related changes in mitochondrial ROS formation.

References

- 1) Nabben M, Hoeks J, Moonen-Kornips E, van Beurden D, Briedé JJ, Hesselink MK, Glatz JF, Schrauwen P. Significance of uncoupling protein 3 in mitochondrial function upon mid- and long-term dietary high-fat exposure. *FEBS Lett.* 585 (2011) 4010-4017.
- 2) Nabben M, Hoeks J, Briedé JJ, Glatz JF, Moonen-Kornips E, Hesselink MK, Schrauwen P. The effect of UCP3 overexpression on mitochondrial ROS production in skeletal muscle of young versus aged mice. *FEBS Lett.* 582 (2008) 4147-4152.

EPR studies of endogenous radicals in human skin.

E. van Faassen¹ and C Suschek²

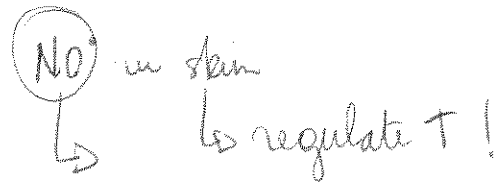
¹ Dept. of Nephrology, Leiden University Medical Centre, Leiden - NL

² Dept. of Trauma and hand surgery, Heinrich Heine University Hospital, Düsseldorf - FRG

NO -> feeling of warmth.
very local generation of heat.

Hemodynamic and vascular disorders usually associate with insufficient levels of the potent vasodilating free radical nitric oxide (NO). Using spin trapping EPR spectroscopy, we provide the first unequivocal detection and quantification of endogenous NO production in human skin biops. We demonstrate significant enhancement of NO levels upon illumination of skin with UVA and even visible light. In addition, UVA illumination induces formation of a multitude of photolytic radical products that promote unwanted oxidation reactions. The underlying photolytic reactions are catalyzed by trace metal ions, in particular endogenous Cu(I) ions in the skin.

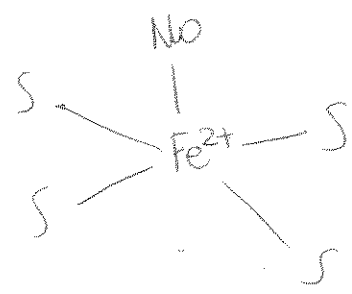
We apply our methods to investigate therapeutic interventions to rescue hemodynamic disorders in human skin. We show that endogenous NO insufficiency may be rescued by application of skin cream spiked with nitrite anions *in vitro* and *in vivo*. As a clinically relevant application, we present the rescue of an acute perfusion failure in the skin transplant of a burn-injury patient.



woundhealing antiseptic (bacteria do not like NO)

concentrations low 0.1 - 20 nMolar
200 nM -> optic shock

Spin trapping NO - Fe²⁺ Nitroxyl radical



very selective

bestraling
Biops
reconstructive surgery

Effect of solar radiation -> UV exposure
(+ Nitrite)

Melanin -> dark pigment
red color, inflammation reaction
to nucleobases! genome.
-> exposure to sun -> stimulates synthesis
DNA photooxidation (UVB) -> UVA

Effects of synthesis conditions on properties of ethane-bridged periodic mesoporous materials as revealed by spin-probe EPR

Feng Lin,^{a,b} Pegie Cool,^b Sabine Van Doorslaer,^a

^a*Department of Physics, University of Antwerp, Antwerp, (Belgium).*

^b*Department of Chemistry, University of Antwerp, Antwerp, (Belgium).*

E-mail: Feng.Lin@student.ua.ac.be

Nanoporous materials are of great importance for applications in the field of sorption and catalysis. Since the 90's, there has been an explosive growth in the development of new ordered mesoporous silicas (pore diameters between 2 and 50 nm). However, for sorption and catalytic applications it is necessary to activate the mesoporous silica structures. One of the most effective ways is to incorporate organic functionalities directly into the silica structure, leading to the materials which is so-called PMOs. Different from the organically functionalized mesoporous silicas, the inorganic and organic moieties are covalently linked to each other and homogeneously distributed in the framework of PMOs, which indeed have extended the research of mesoporous materials from "chemistry of the void space" to the "chemistry of the walls". The combination of the organic and inorganic components of the novel hybrid mesoporous materials endow PMOs with unique chemical, mechanical, catalytic, sorption and electrical properties. Numerous potential applications exist for hybrid organic-inorganic porous materials, e.g. in the chemical industry (catalysis), in environmental applications (metal scavenging) and in medical applications (controlled drug release). However, for further tuning and improving the structural characteristics of these promising hybrid mesostructured materials, it is important to understand the formation mechanism of these materials.

Here, we show that electron paramagnetic resonance (EPR) is an excellent tool to obtain mechanistic insight into the mesoporous materials. On the one hand, by adding spin probes to the synthesis mixture, these probes will function as EPR spy molecules that can monitor the changing structure of the material during the synthesis process. It allows us to elucidate the formation mechanism of the PMO materials. On the other hand, spin probes can also be adsorbed onto the surface of the surfactant-free PMO materials. The analysis of the EPR spectra allows the extraction of structural, mobility and polarity information of the spin probes which will further reflect the pore size, the accessibility, as well as the surface properties of the materials.

Nitroxide spin labels for in-cell EPR

Constantz.

Mykhailo Azarkh

Department of Molecular Physics, Leiden University, Leiden, The Netherlands

Spin-label electron paramagnetic resonance (SL-EPR) spectroscopy has become a powerful and useful tool for studying structure and dynamics of biomacromolecules. However, utilizing these methods at physiological temperatures for in-cell studies is hampered by reduction of the nitroxide spin labels and thus short half-lives in the cellular environment.

Oocytes from African frog *Xenopus laevis* are widely used model systems in cell- and development-biology; here, they were utilized for evaluation of spin labels for in-cell EPR. Reduction kinetics of two structurally different nitroxides has been investigated in cell extracts of *Xenopus laevis* oocytes using rapid-scan cw-experiments at X-band. The five membered heterocyclic ring nitroxide PCA (3-carboxy-2,2,5,5-tetramethylpyrrolidinyl-1-oxy) features much higher stability against intracellular reduction than the six membered ring analog TOAC (2,2,6,6-tetramethylpiperidine-N-oxyl-4-amino-4-carboxylic acid). The analysis of the kinetic data using the Michaelis–Menten model is given and suggests an enzymatic or enzyme-mediated reduction process.

An approach to determine the proper incubation time for in-cell distance measurements is illustrated on the example of human telomeric DNA. Usage of intact cells and cell extracts is discussed.

Literature:

1. M. Azarkh, O. Okle, P. Eyring, D.R. Dietrich, M. Drescher, *J. Magn. Reson.* **2011**, 212, pp. 450-454.
2. M. Azarkh, V. Singh, O. Okle, D.R. Dietrich, J.S. Hartig, M. Drescher, *ChemPhysChem* **2012**, 13, pp. 1444-1447.
3. M. Azarkh, V. Singh, O. Okle, I.T. Seemann, D.R. Dietrich, J.S. Hartig, M. Drescher, *Nat. Protoc.* **2013**, 8, pp. 131-147.

Single-crystalline arrays of thermally oxidized Si nanowires studied by electron spin resonance: the influence of nanowire diameter

M. Jivănescu¹, A. Stesmans¹, and R. Kurstjens²

¹Department of Physics and Astronomy, University of Leuven, Celestijnenlaan 200 D, 3001 Leuven, Belgium

²IMEC, Kapeldreef 75, 3001 Leuven, Belgium

The ever increasing worldwide energy needs in combination with ecological considerations drive enhanced efforts in more and more power generation being obtained from sustainable sources like solar energy. In this strive, silicon as basic material, remains in the run for the production of low-cost high-efficiency solar cells, although the band gap of bulk Si (≈ 1.1 eV) appears not optimal. However, one may attempt to improve on this through quantum confinement (QC) induced band gap widening, e.g., through stepping to designs based on Si nanowires (NWs) thinner than 10 nm [1]. Accordingly, crystallographic ordered Si pillars were lithographically etched into (100)Si wafers and have been thinned down to the intended diameter (Φ) by thermal oxidation, leading to crystallographically ordered arrays of Si NWs that are thoroughly explored for the development of solar cells with enhanced efficiency. However, inhomogeneities in the manufacturing procedure introduce variation in the NWs Φ , decreasing from the center (NWs with top and bottom average diameters of $\Phi_t \approx 15$ and $\Phi_b \approx 32$ nm; sample A) to the edge of the wafer. At half radius one obtains NWs with $\Phi_t \approx 5$ and $\Phi_b \approx 19$ nm (sample B), the lower part tapering upwards quite rapidly, as shown in Fig. 1.

As is the case for any solar cell functionality, the quality of crucial interfaces is vital, which has been addressed by low-temperature electron spin resonance (ESR) measurements. The results indicate a very large density of angle dependent P_b -type defects, mainly P_{b0} (modeled as $Si_3=Si\bullet$), at the very Si NW/SiO₂ interface [2], amounting to $[P_{b0}] \approx 3.9 \times 10^{12} \text{ cm}^{-2}$. We obtain similar P_{b0} densities, even a bit larger for sample A, indicating a similar interface quality in both cases. Thus we infer that the stress levels induced by the thermal oxidation thinning and the particular NW faceting obtained are the much similar, irrespective of the attained Φ . The P_{b0} defects are well known charge traps and non-radiative recombination centers, thus drastically affecting the basic properties of the structure fabricated by this method and its incorporation in solar cell devices. The suppression/elimination of these defects to subcritical levels is primordial for successful solar cell operation.

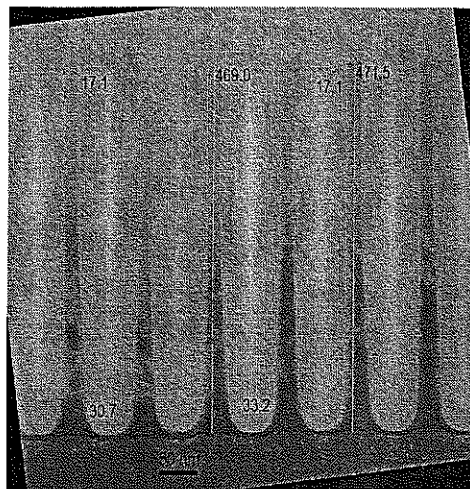


Fig. 1: TEM image of Si NWs at the center of the (100)Si wafer.

References

- [1] D. D. Ma, C. S. Lee, F. C. K. Au, S. Y. Tong, and S. T. Lee, *Science* **299**, 1874 (2003).
- [2] M. Jivănescu, A. Stesmans, and R. Kurstjens, *Jpn. J. Appl. Phys.* **52**, 041301 (2013).

The type 1 copper site of pseudoazurin

Edgar J.J. Groenen, Freek Broeren, Peter Gast, Takamitsu Kohzuma, and Silvia Sottini
Molecular Nano-Optics and Spins, Huygens Laboratory, Leiden University, Leiden, The
Netherlands

The type 1 copper site of proteins and enzymes carries a characteristic set of ligands. Two histidine nitrogens, a cysteine sulfur and a more weakly bound methionine sulfur make up for a trigonal coordination of copper in the oxidized protein that deviates strongly from the tetragonal coordination commonly observed for small inorganic Cu(II) complexes. For long the discussion was whether this structure was a direct consequence of the specific set of ligating amino acids or was imposed by the protein matrix. Around 2000, the debate seemed to be settled following extensive spectroscopic (optical and EPR) and quantum-chemical studies. The ligands are decisive, while subtle variations from protein to protein depend on the second and further coordination spheres. These small structural variations result in significant differences of the electronic structure and thereby tune the electron-transfer properties of the copper site.

During the last years, observations for a few type 1 copper proteins reanimated the discussion. These observations in particular concerned the protein pseudoazurin, both UV/Vis, resonance Raman, and 9 GHz EPR spectroscopy. The structure of the copper site of this protein might not be uniquely defined, but indisputable conclusions were difficult to draw. In an attempt to clarify a confusing debate, we applied 275 GHz cw EPR to pseudoazurin and a set of mutants of this protein in which a ligand in the second coordination sphere was replaced.

In the talk I will describe the variation in the (electronic) structure of type 1 copper sites and introduce the dilemma as regards the copper site of pseudoazurin. Subsequently, I discuss the EPR results at 275 GHz, and show that the increased resolution at 275 GHz as compared to 9 GHz pays. This once more illustrates that "Casimir was right".

Poster presentations

Formation of Nitrosylated Hemoglobin in Human Venous Blood as Surrogate Index of Vascular Endothelial Function.

I. Lobysheva¹, P. Biller¹, F. Dei Zotti¹, B. Gallez³, C. Beauloye², J.L. Balligand¹

(1) Pole of Pharmacology and Therapeutics, (2) Pole of Cardiovascular Pathology, Institute de Recherche Experimentale et Clinique, and (3) Magnetic Resonance Unit, Louvain Drug Research Institute, Université Catholique de Louvain, Brussels, Belgium

Nitric oxide binding to deoxygenated hemoglobin (Hb) results in formation of different paramagnetic species of heme-nitrosylated Hb depending on NO-hosting subunits and Hb conformation. Two forms were predominantly observed in blood: 5-coordinate- α -HbNO (T-form, deoxy-like) and 6-coordinate- α -HbNO (R-form, oxy-like) due to appropriately low stability of nitrosylated β -heme adducts (6-coordinate- β -HbNO, R-form, oxy-like). We hypothesized that erythrocyte level of nitrosylated hemoglobin (5-coordinate- α -HbNO) reflects bioavailability of vascular endothelial NO in venous blood as well as vascular endothelial function *in vivo*.

Accurate interpretation of the EPR signals in human blood has remained a challenge due to overlapping EPR signals originating from different paramagnetic species in the region 3000-3400 Gauss (X-band, $g \sim 2.06-1.9$). Remarkably, a typical EPR spectrum of 5-coordinate nitrosyl-heme (α -Hb) that is predominantly observed in venous blood, displays the well-resolved triplet hyperfine (hf) structure at $g_z \sim 2.01$ ($A_N \sim 16.8$ G) due to net donation of electron density from Fe(II) to NO after cleavage of the bond between the heme iron and the proximal His residue of the R-form. We developed a modified EPR subtraction approach specifically designed for digital subtraction of the EPR signal of protein-centred free radical species ($g \sim 2.005$, with individually fluctuating peak-to-peak width $\sim 16-19$ G) to reveal the triplet hf structure of the T-form of HbNO in snap-frozen red blood cells (RBCs) isolated by centrifugation (800xg, 10 minutes) from human venous blood immediately after collection in vacuum tubes to keep venous oxygen level. The spectrum for subtraction of overlapping signals was obtained for each subject as difference spectrum between two RBC samples treated and non-treated with antioxidant (ascorbic acid, 10 mM, 15 minutes after 30-minute exposition of samples to open air) for reduction of protein-centered free radicals. The calibration curve was generated using HbNO complexes, synthesized in isolated RBCs after incubation with mixture of sodium nitrite at different concentration and sodium dithionite ($\text{Na}_2\text{S}_2\text{O}_4$, 20 mM) in anaerobic condition (1% of O_2 ; RUSKINN workstation INVIVO₂400; 37°C). Strict linearity was observed for the proportional increase of either the intensity of HbNO EPR signal obtained by signal double integration, or the amplitude of first hf component ($g_z \sim 2.01$) with increasing concentrations of added nitrite. The double-integrated intensities of the EPR signals were normalized by that of known EPR standards (Cu-EDTA complex, 50 μM frozen in 30% glycerol).

Using this method, we examined whether the quantified erythrocytic levels of 5-coordinate- α -HbNO formed *in vivo* correlate with endothelial function assessed from the peripheral vasodilator response to reactive hyperemia (RH) by peripheral arterial tonometry (PAT), in a group of healthy volunteers. We observed mean erythrocyte HbNO concentration (5-coordinate nitrosyl-heme, α -Hb) in group of healthy volunteers of 219 ± 12 nmol/L ($N = 50$) with a dynamic increase of HbNO levels in erythrocytes isolated at 1-2 min of post-occlusion hyperemia ($120 \pm 8\%$ of basal levels). Post-occlusion HbNO levels were correlated with basal levels. Both basal and post-occlusion HbNO levels were significantly correlated with RH indexes ($r = 0.58$; $P < 0.0001$ for basal HbNO).

Conclusion: The study provides the first demonstration of quantitative measurements of 5-coordinate- α -HbNO in human venous blood, its dynamic physiologic regulation and significant correlation with endothelial function measured by tonometry during hyperemia that opens the way to further understanding of *in vivo* determinants of NO bioavailability in human circulation.

Optically detected magnetic resonance study of NV⁻ centers in diamond

Boris Yavkin, Shashi Singham, Etienne Govaerts

Department of Physics, University of Antwerp, Antwerp, (Belgium).

This work represents first preliminary results of our group concerning optically detected magnetic resonance (ODMR) in diamond's famous NV⁻ centers. These centers currently attract attention as a possible realization of a solid-state microscopic magnetic field sensor. We recorded ODMR spectra from a few diamonds, under different conditions of laser and MW power, as well as in zero and small static or variable external magnetic field.

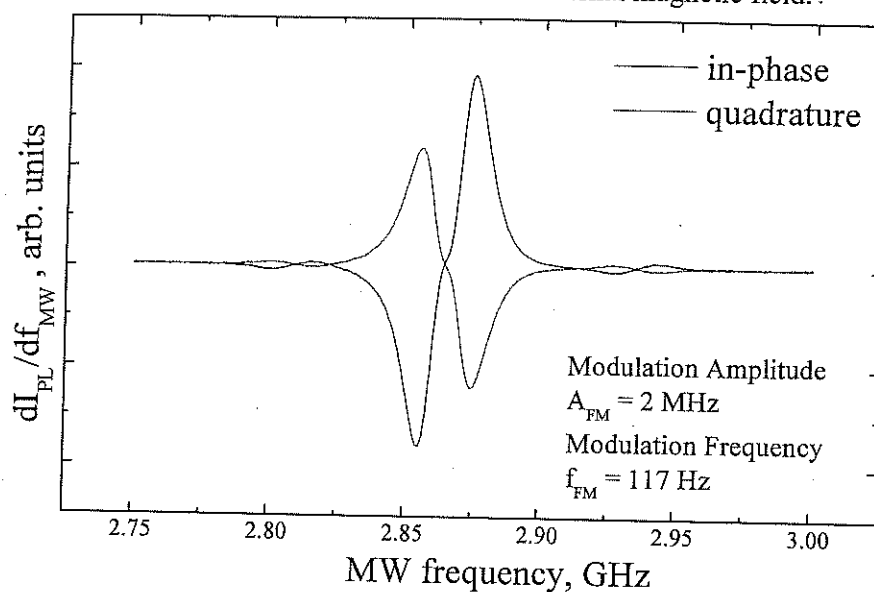


Fig.1. ODMR spectrum detected by frequency modulation of excitation light

Optical and MW parts of setup have been built, and data acquisition software has been written in MATLAB. In our setup, we are using 532nm Nd³⁺:YAG laser with output power up to 180mW and MW generator up to 3.2 GHz in frequency and maximum 1W of power.

Now we are testing our setup for sensitivity limit which should be below 0.1mG to serve as a robust magnetic field detector for biological application.

Q-band EMR study of radicals in X-irradiated L-threonine

Gauthier Vanhaelewyn, Henk Vrielinck and Freddy Callens

Department of Solid State Sciences, Ghent University
Krijgslaan 281 – S1, 9000 Gent, Belgium

Electron Magnetic Resonance (EMR) is a prominent research tool for detecting, quantifying and identifying radiation-induced paramagnetic defects in organic (poly) crystalline materials (amino acids, sugars, sugar phosphates, etc.). This kind of research is motivated, on the one hand by the favorable Electron Paramagnetic Resonance (EPR) dosimetric properties of some organic materials (e.g., alanine and sucrose), and on the other hand by the need to understand the radiation effects in biological molecules (e.g., DNA and proteins).

In the past decennia radiation-induced radicals were successfully identified in amino acids (alanine, glycine, lysine, arginine, serine phosphate, etc.) and sugars (sucrose, fructose, sorbose, glucose phosphate, trehalose dehydrate, etc.). Hence, the number of accurately studied systems gradually increases to a level that might reveal underlying principles with respect to the formation of certain types of radicals.

An EMR study of the X-irradiated amino acid L-threonine ($\text{CH}_3\text{CH}(\text{OH})\text{CH}(\text{NH}_3^+)\text{COO}^-$) reveals promising results for dosimetric applications and fundamental research. Its chemical structure is similar to that of alanine ($\text{CH}_3\text{CH}(\text{NH}_3^+)\text{COO}^-$). In this respect, radiation defects in L-threonine might straightforwardly be compared with the extensively studied L-alanine radicals. In this study, the hyperfine coupling (HFC) tensors of the observed radicals in RT X-irradiated L-threonine single crystals were determined at RT and 20 K using Electron Nuclear Double Resonance (ENDOR) comparable to the experiments on alanine. Four different radicals were observed at 20 K and three of their counterparts at RT. One of these radicals, exhibiting several β -HFCs, is clearly prevailing in the EPR spectrum. This dominant contribution in L-threonine seems to originate from the H-abstraction radical ($\text{CH}_3\dot{\text{C}}(\text{OH})\text{CH}(\text{NH}_3^+)\text{COO}^-$) with negligible ^{14}N coupling. In another EPR study of γ -irradiated crystals of DL-threonine at RT the same radical model ($\text{CH}_3\dot{\text{C}}(\text{OH})\text{CH}(\text{NH}_3^+)\text{COO}^-$) was proposed for the dominant EPR signal^[1]. However, in that case a significant ^{14}N HFC (≈ 13 MHz) was observed. Careful analysis reveals that the dominant radical in DL-threonine, exhibiting the ^{14}N HFC, is most probably one of the less abundant radical in L-threonine. A third detected radical exhibits a strong α -HFC and was tentatively assigned to the amino abstracted radical $\text{CH}_3\text{CH}(\text{OH})\dot{\text{C}}\text{HCOOH}$. In alanine the amino abstracted radical makes the dominant contribution to the spectrum.

[1] D. M. Close and R. S. Anderson, EPR of γ -irradiated crystals of DL-threonine at room temperature. *J. Chem. Phys.*, 60(7), 2828-2831 (1974).

Inherent interface defects at the thermal (211)Si/SiO₂ interface

S. Iacovo and A. Stesmans

Semiconductor Physics Laboratory, Department of Physics and Astronomy, University of Leuven, Celestijnenlaan 200 D, B-3001 Leuven, Belgium

Stimulated by advancements in Si-based devices and nanostructures, an extensive multifrequency electron spin resonance (ESR) study has been carried out as a function of oxidation temperature T_{ox} (400-1066 °C) on the thermal (211)Si/SiO₂ interface in terms of occurring intrinsic paramagnetic point defects. As reported in the literature, (211)Si wafers are used as substrates for the epitaxial growth of CdTe/HgCdTe/GaAs stacks [1,2] for solar cell applications. Also, substantial (211)boundary faceting is naturally encountered in some particular growth of Si nanowires [3]. These observations would thus reflect the need of an in depth understanding of (211)Si facets, especially in connection with the interface it forms with its natural oxide, SiO₂.

Conventional cw K-band and Q-band measurements have been performed at low temperatures (~4.3K) to atomically identify the types of intrinsic point defects occurring at the (211)Si/SiO₂ interface. Full angular characterization of the defects has been carried out for the applied magnetic field **B** rotating in the [01-1] plane.

The main types of interface defects observed are P_b-type centers, closely related to the P_b⁽¹¹¹⁾ and P_{b0}⁽¹⁰⁰⁾ variants characteristic for the (111) and (100)Si/SiO₂ interfaces, respectively, that is, interfacial Si dangling bond (DB) defects (generic entity Si₃≡Si^{*}, where the dot represents an unpaired electron located in an unpaired interfacial sp³ hybrid). Two species are observed: A dominant one of axial symmetry with the Si DB along the [111] direction, pointing into the SiO₂ layer, at 19.5° with the [211] interface normal, giving rise to a one branch g map characterized by the principal g values $g_{\parallel}=2.0022$ and $g_{\perp}=2.0079$ for $T_{\text{ox}}\sim 400$ °C. Q-band saturation spectroscopy measurements have enabled to reveal a ²⁹Si hyperfine doublet centered at the central Zeeman line, identifying the defect as an unpaired electron with strongest interaction with a single Si nucleus. On the basis of comparison of its pertinent ESR parameters, it is typified as P_{b0}⁽²¹¹⁾ variant. A second, less intense (~9 ×) variant corresponds to Si DBs along the equivalent [1-11] and [11-1] directions pointing out of the (211)Si surface.

For low T_{ox} (<500 °C), a total P_b-type defect density of $\sim 1 \times 10^{13}$ cm⁻² is observed, gradually declining to the plateau value $\sim 4.2 \times 10^{12}$ cm⁻² for $T_{\text{ox}} \rightarrow 800$ °C. This means, compared to the other thermal Si/SiO₂ structures, an inherent interface quality about 2 times worse than the preferred and technologically dominant (100)Si/SiO₂ one, but comparable to the (110)Si/SiO₂ one. As a main conclusion, a $T_{\text{ox}} \geq 800$ °C is thus required to attain the minimum P_b-type interface defect density.

References

- [1] C. Fulk et al., J. E. M. **35**, 1449 (2006)
- [2] S. Hosseini Vajargah et al., J. Appl. Phys. **112**, 093103 (2012)
- [3] V. Schmidt et al., Chem. Rev. **110**, 361 (2010)

**ODMR study of formation of triplet state in PCBM
via photoinduced charge transfer
in Super Yellow PPV: PCBM blend films**

Biniam Zerai Tedlla¹, Zhu Feng², Janssen Paul², Bert Koopmans², Etienne Goovaerts¹

1. Department of Physics, University of Antwerpen, Universiteitsplein1, B-2610, Wilrijk, Antwerpen, Belgium
2. Physics of Nanostructures, Dept. of Applied Physics, Eindhoven University of Technology, P.O. Box 513, NL-5600 MB Eindhoven, The Netherlands

Owing to low dielectric constant, photoexcitation in organic semiconductor materials results in bound electron-hole pair called exciton. Recently in polymer:PCBM solar cell, the presence of an intermediate interfacial charge transfer (CT) ground state, with short lifetimes at the interface between the polymer and the PCBM phases, was demonstrated by using different experimental techniques [1-3]. It is proposed in polymer:PCBM solar cells that, depending on the energy level of this CT state relative to the singlet and triplet energy levels of the constituent materials, the CT state could decay to the lowest energy triplet state of the polymer or the PCBM [5]. Using optically detected magnetic resonance (ODMR) technique in blends of PPV-polymers with the fullerene derivative PCBM, we detect the triplet ODMR signature of PCBM in SY-PPV:PCBM blend films, while it is absent in MDMO-PPV:PCBM blend films. We concluded that the ODMR detected PCBM triplet state in SY-PPV:PCBM blend film is generated via the CT state, rather than due to a direct absorption of photon by the PCBM molecule. The absence of the ODMR triplet signature of PCBM in MDMO-PPV:PCBM film supports the argument of direct dissociation of CT states to free charges claimed based on energy band alignment [1,4].

- [1] D. Veldman et al., *Adv. Func. Mater.*, 19, 1939-1948 (2009)
- [2] M. C. Scharber et al., *Phys. Rev. B* 67, 085202 (2003)
- [3] J. Behrends et al., *Phys. Rev. B* 85, 125206 (2012)
- [4] J. J. Benson-Smith et al., *Adv. Func. Mater.*, 17,451-457 (2007)
- [5] B.C.Thompson, and J. M. J. Frechet, *Angew. Chem. Int. Ed.*, 58-77 (2008)

Comparison of human and icefish neuroglobin and cytoglobin

B. Cuypers¹, W. Van Leuven², S. Vermeyleylen², S. Dewilde², and S. Van Doorslaer¹

¹SIBAC Laboratory, Department of Physics, University of Antwerp

²PPES Laboratory, Department of Biomedical Sciences, University of Antwerp
Universiteitsplein 1, B-2610 Antwerp, Belgium

Neuroglobin and cytoglobin are two recently discovered globins which have been identified in mammalian and non-mammalian vertebrates. In this work, icefish neuroglobins and cytoglobins are investigated using electron paramagnetic resonance (EPR) and compared to earlier findings about the human variants.¹ The neuro- and cytoglobins of the icefishes *Dissostichus mawsoni* and *Chaenocephalus aceratus* are analysed. These two species are chosen because in contrast to *D.maw*, *C.ace* has white blood and lacks both myo- and hemoglobin. In human neuroglobin, the presence of an intramolecular disulfide bond between two cysteines in the CD loop (CD7-D5) is found to modulate the gas binding affinity through a change in the heme-pocket structure.² In human cytoglobin, a negligible effect of disulfide bridge formation on the gas binding kinetics is observed.² The investigated icefish neuroglobins and cytoglobins differ from their respective human forms in their cysteine positions. It is shown that no effect of a possible intramolecular disulfide bond on the heme-pocket structure is observed for both the icefish neuroglobins and cytoglobins. The icefish cytoglobins however do form an intermolecular bond that also results in an alteration of the heme-pocket structure as follows from the EPR results.

¹E. Vinck, S. Van Doorslaer, S. Dewilde and L. Moens, "Structural change of the heme pocket due to disulfide bridge formation is significantly larger for neuroglobin than for cytoglobin," *J. Am. Chem. Soc.*, 126, 4516-4517, 2004.

²D. Hamdane, L. Kiger, S. Dewilde, B. Green, et al., "The redox state of the cell regulates the ligand binding affinity of human neuroglobin and cytoglobin," *J. Biol. Chem.*, 278, 51713-51721, 2003.

EPR study of point defects in thermal GaAs/GaAs-oxide structures

S. Nguyen, V. V. Afanas'ev, and A. Stesmans

*Semiconductor Physics Laboratory, Department of Physics, University of Leuven,
3001 Leuven, Belgium*

In an attempt to atomically assess interface and oxide-related point defects, an extensive Q band (34 GHz) low-temperature electron spin resonance study has been carried out on semi-insulating (Fe compensated) GaAs/oxide structures, implying both powders and (100)GaAs/oxide slices, thermally grown in the range $T_{\text{ox}}=350-615$ °C. Various spectra are observed as result of thermal oxidation:

As for powders, a way to enhance the effective sample (interface) area, this includes the prominent 4-line EL2 defect spectrum centered at $g\sim 2.043$ and characterized by the isotropic hyperfine constant $A_{\text{iso}}\sim 910$ G, ascribed to the $^{75}\text{As}_{\text{Ga}}^+$ antisite defect. Observed in freshly crushed powder, it substantially increases in density with oxidation, herewith revealing interfacial As enrichment as endemic to thermal oxidation of GaAs resulting in poor interface quality, in line with theoretical prognosis. With this observation, first atomic identification is thus provided of the generation and the presence at the thermally grown GaAs/oxide interface of a defect known to operate as a detrimental electrically active deep level center. The maximum defect density, of the order of 10^{13} centers/cm², is reached for $T_{\text{ox}}\sim 440$ °C. As more device-relevant confirmation, the defect is also observed in thermal (100)GaAs/oxide slices.

Two more isotropic signals are observed: In the as-oxidized powders, a first one is observed at $g\sim 2.063$, while a second one is detected at $g\sim 1.937$ in powders oxidized in the range $T_{\text{ox}}=510-615$ °C; but only after additional VUV irradiation; It may originate from As clusters.

None of the above signals is observed on the virgin as-received parent c-(100)GaAs wafer; Yet, from the substrate material we additionally observe the 5-branch spectrum of substitutional Fe impurities (spin $S=5/2$) in GaAs, with inferred crystal field constant $a\sim 360$ G, well in line with previous observations. The results are confronted with advanced theoretical interface and defect models.

Electron paramagnetic resonance spectrometry and imaging in melanomas: A comparison between pigmented and nonpigmented human malignant melanomas.

Quentin Godechal¹, Ghanem Ghanem², Martin Cook³, and Bernard Gallez¹

¹Biomedical Magnetic Resonance, University of Louvain, Brussels, Belgium, ²Universite libre de Bruxelles, Brussels, Belgium, ³Department of Histopathology, Royal Surrey County Hospital, Guildford, United Kingdom

Purpose:

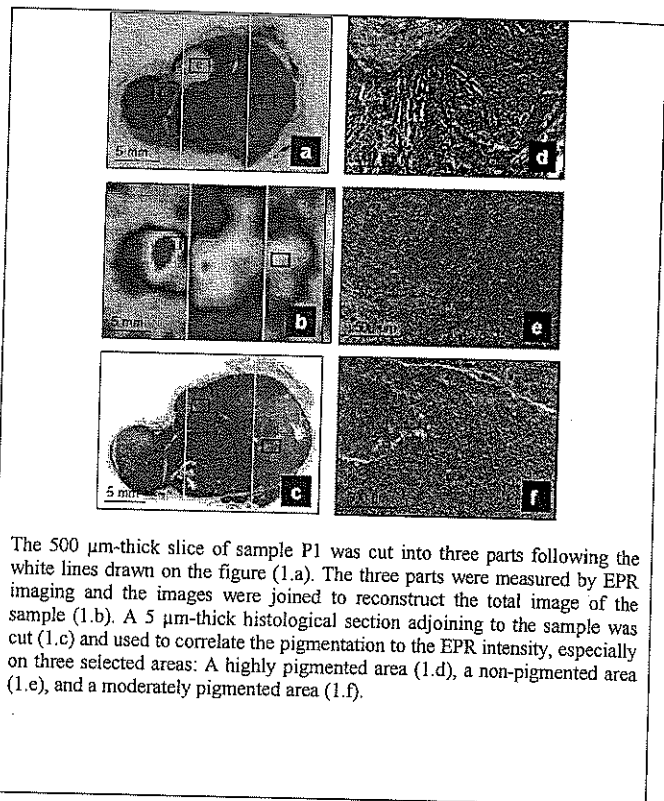
It is known for a long time that the melanin pigments present in normal skin, hair and most of malignant melanomas (1-3) can be detected by electron paramagnetic resonance (EPR) spectrometry. In this study, we proposed to use EPR imaging as a tool to map the concentration of melanin inside *ex-vivo* human pigmented and non-pigmented melanomas and to correlate this cartography with anatomo-pathology.

Methods:

Six paraffin-embedded human melanoma samples were analyzed. The samples were classified as highly pigmented ($n = 3$) or non-pigmented ($n = 3$) on the basis of the histological findings. A 500- μm -thick slice was cut from each melanoma. Each of the six slices was then cut into 2 or 3 parts due to the small size of the X-Band EPR cavity used for the EPR Imaging measurement. All spectra and images were recorded at room temperature on a Bruker E540 Elexsys system (Bruker Biospin, GmBh) equipped with a Super High Sensitivity Probe (10mm diameter, 30 mm long) operating in X-band mode at approximately 9.5 GHz and 100 KHz modulation frequency. For images, the following parameters were used: microwave power: 3.2 mW; modulation amplitude: 0.25 mT; conversion time: 10.24 ms; time constant: 5.12 ms; field of view: 23 mm; sweep width: 182 G; number of points: 1024; number of scans: 5; sweep time: 10.49 s; gradient field: 450 mT/m; number of projections: 29; pixel size: 0.6 mm; total acquisition time: 32.5 min. For each sample, a 5- μm -thick section, contiguous to the 500- μm -thick used for EPR, was processed for histology (hematoxylin-eosin staining). The histological sections were then scanned with a Zeiss Mirax microscope.

Results:

Globally, each part of the pigmented samples allowed the successful acquisition of an EPR image. All the EPR images closely reflected the shape and size of their respective sample. Accurate measurements of the dimensions showed a mean difference of 1.15% between the samples and their respective images. For the three samples, the EPR intensity in a given area was unambiguously correlated to the presence or absence of melanin pigments. To illustrate this observation, three different areas were selected on one sample P1 on the basis of the concentration of melanin visible on the histological section. A highly pigmented area was found on the left part of the sample and is presented on figure 1.d. A totally non pigmented area was found in the upper side of the middle part and is presented on figure 1.e. Finally, a moderately pigmented area was taken from the right part of the sample and is presented on figure 1.f. On the EPR image, these three areas were linked to three areas with highly different intensities, the non pigmented area being impossible to distinguish from the background and the highly pigmented area exhibiting the strongest intensity. In opposition, no EPR signal coming from melanin was observed from non pigmented melanomas, demonstrating therefore the absence of EPR detectable pigments inside these particular cases of skin cancer and the importance of the pigmentation for further EPR imaging studies on melanoma.



The 500 μm -thick slice of sample P1 was cut into three parts following the white lines drawn on the figure (1.a). The three parts were measured by EPR imaging and the images were joined to reconstruct the total image of the sample (1.b). A 5 μm -thick histological section adjoining to the sample was cut (1.c) and used to correlate the pigmentation to the EPR intensity, especially on three selected areas: A highly pigmented area (1.d), a non-pigmented area (1.e), and a moderately pigmented area (1.f).

Conclusion:

The importance of the pigmentation for EPR measurement was unambiguously demonstrated. Moreover, EPR images accurately reflected the distribution of melanin pigments within melanoma samples.

References:

- 1) E. Vanea et al, *NMR Biomed* 2008;21:296-300; 2) Q. Godechal et al, *Contrast Media Mol Imaging* 2011;6:282-288; 3) Q. Godechal et al, *J. Skin Cancer* 2011, 2011:273280; 4) Q. Godechal et al, *Exp Dermatol* 2012;21:341-346.

The large in vitro heterogeneity of chlorite dismutase of *Magnetospirillum* sp strain Lusitani

A. De Schutter¹, D. Freire², P. González², S. Van Doorslaer¹

¹SIBAC laboratory, department of Physics, University of Antwerp, Belgium

²REQUIMTE, department of Chemistry, Faculty of Science and Technology, Universidade Lisboa Nova

Chlorite dismutase (cld) is a heme-containing enzyme capable of catalyzing ecotoxic ClO_2 in to Cl^- and O_2 . Cld has been purified from the chlorate reducing bacterium *Magnetospirillum* sp and was investigated with spectroscopic techniques. Numerous low spin (LS) and high spin (HS) heme species were found using continuous wave EPR (CW-EPR) suggesting a natural flexibility of the enzyme. The presence of the different LS heme species in cld stem from different distal ligations. Most of the LS species could be attributed to OH ligation to the heme or a biological non relevant form but one LS heme specie, referred to as LS 1, is intriguing. LS 1 is similar to the LS heme specie found by Thorrell et al. and de Geus et al. for recombinant cld of *A. oryzae* and *I. dechloratans* respectively [1], [2]. They suggested a distal ligation of Fe(III) by a histidine or imidazole-like molecule. Our extended pulsed EPR analysis of LS 1 compared to cld after addition of imidazole showed that this ligation form is not present in LS 1.

ESR dating of Neogene marine sands from the southern North Sea basin, NE Belgium: first results

Beerten K.¹, Iacovo S.², Jivanescu M.², Stesmans A.², Vandenberghe N.³

¹ SCK-CEN, Institute Environment-Health-Safety, Mol, Belgium

² Department of Physics, KULeuven, Leuven, Belgium

³ Department of Earth and Environmental Sciences, KULeuven, Leuven, Belgium

In recent years, the electron spin resonance (ESR) dating method has been applied to buried sediments that range in age between ~ 100 ka and several Ma. The method is based on the measurement of accumulated radiation damage in quartz crystals during burial, and can thus in theory be applied to obtain absolute numerical age control on any quartz-rich sediment given several conditions are met. The most important of these is sunlight bleaching of pre-existing radiation damage prior to burial. In this case study, we present preliminary ESR dating results of three samples from a cored borehole in Miocene glauconite-rich sands, which are expected to have been deposited prior to 7.5 Ma.

Following chemical and physical purification of the samples (taken at 107 m, 135 m and 147 m depth), quartz grains (100-200 μm) were irradiated by Co-60 gamma rays to doses between 1-150 kGy. Individual aliquots (each weighting several 100 mg) were measured at cryogenic temperatures in a JEOL X-band ESR spectrometer operating at a microwave frequency of ~ 9.2 GHz. Defect densities were derived by integration of relevant ESR spectra, and making use of a comounted defect density calibrated marker sample. Subsequently, the equivalent dose was calculated using the thus constructed dose curves (including the natural, unirradiated, aliquot). Finally, dose rates were determined using high resolution gamma ray spectrometry in the laboratory.

ESR measurements allowed to identify three different species, including the AlO₄, Ti-Li and E'-center. Overlapping of the AlO₄ signal with other signals, and the generally poor bleaching characteristics of the E'-center led to the use of Ti-Li impurity centers for dating. Dose curves of the latter typically showed radiation saturation around doses of up to several 10 kGy, after which the ESR intensity tends to decrease quickly. Polynomial, exponential growth and linear functions were fitted to the dose curve data points, leading to equivalent dose estimates ranging between 3 kGy and 7 kGy. Given measured dose rates between 2-3 kGy/Ma, ESR ages of all three samples are younger than 4 Ma, and thus severely underestimate the palaeontological age of these Miocene sands. Two possible reasons for this discrepancy are being considered, involving instability of the Ti-Li signal over such long burial times, and dose rate variations during burial. Further research will concentrate on the potential use of E'-centers, and improved detection of the AlO₄ signal in these samples.

Influence of free radicals signal from dental resins on the radio-induced signal in teeth in nuclear retrospective dosimetry : kinetic analysis using electron paramagnetic resonance.

C. Desmet¹, Ph. Levêque¹, A. DosSantos², J. Leprince^{2,3}, G. Leloup^{2,3} and B. Gallez¹

¹ Biomedical Magnetic Resonance Group, Louvain Drug Research Institute, UCLouvain, ² School of Dental Medicine and Stomatology, UCLouvain, ³ Centre de Recherche et d'Ingénierie en Biomatériaux CRIBIO, UCLouvain.

Purpose

Dental enamel is a natural dosimeter frequently used with EPR detection for retrospective dosimetry purpose and dose reconstruction in individuals accidentally exposed to ionizing radiations, because a dose dependent signal is observed in this type of material [1, 2]. Teeth very frequently bear restoration performed by dentists using dimethacrylate based resins. A strong EPR signal is also documented in those resins, possibly causing an interference with the dosimetric signal from the enamel. The aim of this study was to evaluate the influence of dental resins on the measurement of the dosimetric signal in teeth.

Method

Among the commercial resins the most frequently used in dentistry, 19 were included in this study. Experimental compositions of different common commercial monomers (Bis-GMA, TEGDMA, UDMA, Bis-EMA) were also evaluated to search for a possible class effect. Firstly, the occurrence and magnitude of an EPR signal was investigated in each resin. Secondly, the decay kinetics of the EPR signal was measured over a 6 months period (L and X band). The size of each sample (30mg) was compatible with a medium-size restoration of an anterior tooth. The signal intensity was compared to the dosimetric signal recorded in teeth after a 3 Gy irradiation.

Results

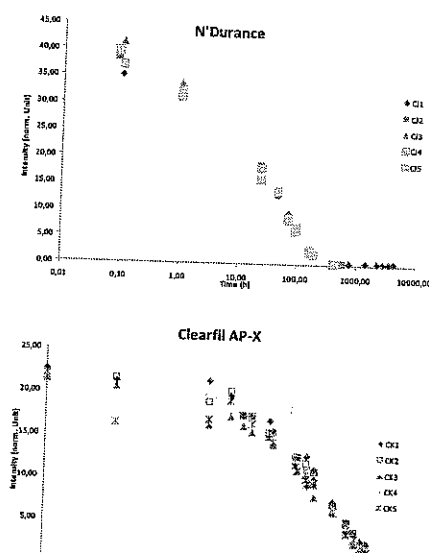


Fig. 1 : Decay kinetics of the epr signal recorded in X band in commercial resins N'Durance and Clearfil AP-X. Time is expressed in a log scale.

An EPR signal was observed in all the samples tested. The initial signal recorded after polymerization ranged from 16 times (i.e. Venus Diamond, Heraeus Kulzer Inc.) to 105 times (N'Durance, Septodont) higher than the dosimetric signal observed in tooth after a 3 Gy irradiation.

The observed decay kinetics followed a bi-exponential model with a first compartment showing a rapid decay and a second compartment showing a much slower decay. In both compartments, different rates of signal decay were observed according to the tested resin. The most rapid decay was seen in N'Durance (Septodont) ($t_{1/2\ 1st} = 1.2\ h\ (1.0-1.7)$; $t_{1/2\ 2nd} = 51\ h\ (47-57)$) and the slowest decay was seen in Clearfil AP-X (Kuraray America, Inc) ($t_{1/2\ 1st} = 82.8\ h\ (58.7-140.4)$; $t_{1/2\ 2nd} = 1270\ h\ (1101-1499)$) (Fig. 1). In most resins, the signal recorded six months after the polymerization was low enough not to interfere significantly with the dosimetric signal.

Conclusion

Tooth enamel associated with EPR detection is a very promising natural dosimeter. When conducting retrospective dosimetry, attention should be paid to recent restorations on teeth (less than 6 months), specially for doses lower than 3Gy. These results should be refined by further studies investigating the influence of size and the geometry of the restoration on the dosimetric signal using "in the field" conditions.

References

1. Trompier F, Bassinet C, Wieser A, De Angelis C, Viscomi D, Fattibene P. Radiation-induced signals analysed by EPR spectrometry applied to fortuitous dosimetry. *Ann Ist Super Sanita*. 2009; 45: 287-296.
2. Iwasaki A, Grinberg O, Walczak T, Swartz H. In vivo measurements of EPR signals in whole human teeth. *Applied Radiation and Isotopes* 2005; 62: 187-190.

List of attendees

- Azarkh Mykhailo**, Department of Molecular Physics, Leiden University, Leiden, The Netherlands
- Beerten Koen**, SCK-CEN, Institute Environment-Health-Safety, Mol, Belgium,
kbeerten@sckcen.be
- Briedé Jacco**, Department of Toxicogenomics, Faculty of Health, Medicine and Life Sciences (FHML) School for Oncology and Developmental Biology (GROW), Maastricht University, PO Box 616, 6200 MD, Maastricht, The Netherlands.
J.Briede@maastrichtuniversity.nl
- Broeren Freek**, MONOS Leiden, Leiden University, Nielsbohrweg 2, 2333 CA Leiden, Huygens building, 8th floor, the Netherlands
- Callens Freddy**, Department of Solid State Sciences, UGent, Krijgslaan 281-S1, 9000 Gent,
freddy.callens@ugent.be
- Cuypers Bert**, Spectroscopy in Biophysics and Catalysis (SIBAC), University of Antwerp, Universiteitsplein 1, 2610 Wilrijk, bert.cuypers@ua.ac.be
- De Preter Geraldine**, Biomedical magnetic resonance research unit (REMA), Université Catholique de Louvain (UCL), 1200 Brussels, geraldine.depreter@uclouvain.be
- De Schutter Amy**, Spectroscopy in Biophysics and Catalysis (SIBAC), University of Antwerp, Universiteitsplein 1, 2610 Wilrijk, amy.deschutter@ua.ac.be
- Dei Zotti Flavia**, FATH, University of Louvain Medical School, Experimental and Clinical Research Institute, 52 Avenue E.Mounier, UCL-FATH 5349, 1200 Brussels,
flavia.deizotti@uclouvain.be
- Desmet Céline**, Biomedical Magnetic Resonance Unit (REMA), Louvain Drug Research Institute, Université Catholique de Louvain, Avenue Mounier 73.08, 1200 Brussels,
celine.m.desmet@uclouvain.be
- Donkersloot Rembrandt**, MONOS Leiden, Leiden University, Nielsbohrweg 2, 2333 CA Leiden, Huygens building, 8th floor, the Netherlands, rembrandtdonkersloot@gmail.com
- Gallez Bernard**, Biomedical magnetic resonance research unit, Université Catholique de Louvain (UCL), 1200 Brussels, bernard.gallez@uclouvain.be
- Gast Peter**, Molecular Nano-Optics and Spins, Huygens Laboratory, Leiden University, Leiden, The Netherlands, gast@physics.leidenuniv.nl
- Groenen Edgar**, Molecular Nano-Optics and Spins, Huygens Laboratory, Leiden University, Leiden, The Netherlands, groenen@physics.leidenuniv.nl
- Goovaerts Etienne**, Experimental Condensed Matter Physics, University of Antwerp, Universiteitsplein 1, 2610 Wilrijk, etienne.goovaerts@ua.ac.be
- Iacovo Serena**, Department of Physics and Astronomy, Semiconductor Physics Laboratory, KU Leuven, Celestijnenlaan 200D-2417, 3001 Leuven, serena.iacovo@fys.kuleuven.be

- Jivanescu Mihaela**, Department of Physics and Astronomy, Semiconductor Physics Laboratory, KU Leuven, Celestijnenlaan 200D-2417, 3001 Leuven, mihaela.jivanescu@fys.kuleuven.be
- Kathiresan Venkatesan**, Biomedical magnetic resonance research unit, Université Catholique de Louvain (UCL), 1200 Brussels, venkatesan.kathiresan@uclouvain.be
- Kepa Jacek**, Department of Physics and Astronomy, Semiconductor Physics Laboratory, KU Leuven, Celestijnenlaan 200D-2417, 3001 Leuven, jacek.kepa@fys.kuleuven.be
- Kumar Pravin**, MONOS Leiden, Leiden University, Nielsbohrweg 2, 2333 CA Leiden, Huygens building, 8th floor, the Netherlands.
- Lin Feng**, Spectroscopy in biophysics and catalysis (SIBAC), University of Antwerp, Campus Drie Eiken, Universiteitsplein 1, 2610 Wilrijk, feng.lin@student.ua.ac.be
- Lobysheva Irina**, FATH, University of Louvain Medical School, Experimental and Clinical Research Institute, 52 Avenue E.Mounier, UCL-FATH 5349, 1200 Brussels, irina.lobysheva@uclouvain.be
- Maduro Luigi**, MONOS Leiden, Leiden University, Nielsbohrweg 2, 2333 CA Leiden, Huygens building, 8th floor, the Netherlands.
- Maurelli Sara**, Dipartimento di Chimica, Università di Torino, via Pietro Giuria 7, 10125 Torino, Italy - Spectroscopy in Biophysics and Catalysis Group, Department of Physics, University of Antwerp, Universiteitsplein 1, 2610 Wilrijk, sara.maurelli@unito.it
- Mouithys Mickalad**, Center for Oxygen, Research & Development (CORD), University of Liège, Institute of Chemistry, B6a Allée de la Chimie, Domaine Universitaire du Sart Tilman, 4000 Liège, amouithys@ulg.ac.be
- Nami Faezeh**, MONOS Leiden, Leiden University, Nielsbohrweg 2, 2333 CA Leiden, Huygens building, 8th floor, the Netherlands, nami@physics.leidenuniv.nl
- Nguyen Sang**, Department of Physics and Astronomy, Laboratory Semiconductor Physics, KU Leuven, Celestijnenlaan 200D-2417, 3001 Leuven, sang.nguyen@fys.kuleuven.be
- Penders Marc**, Bruker Belgium NV, Kolonel Bourgstraat 124 bus 1, 1140 Brussel, marc.penders@bruker.be
- Stesmans André**, Department of Physics and Astronomy, Semiconductor Physics Laboratory, KU Leuven, Celestijnenlaan 200D-2417, 3001 Leuven, andre.stesmans@fys.kuleuven.be
- Van Doorslaer Sabine**, Spectroscopy in biophysics and catalysis (SIBAC) Laboratory, University of Antwerp, Department of Physics, Universiteitsplein 1, 2610 Wilrijk, sabine.vandoorslaer@ua.ac.be
- Van Faassen**, Department of Nephrology, Leiden University Medical Centre, Leiden, The Netherlands, E.E.H.van.Faassen@lumc.nl
- Vanhaelewyn Gauthier**, Electron Magnetic Resonance (EMR) group, Department of Solid State Sciences, Ghent University, Krijgslaan 281-S1, 9000 Gent, Gauthier.vanhaelewyn@ugent.be
- Van Son Martin**, MONOS Leiden, Leiden University, Nielsbohrweg 2, 2333 CA Leiden, Huygens building, 8th floor, the Netherlands, son@physics.leidenuniv.nl

Van 't Hoff Ton, Bruker Nederland BV, Bruynvisweg 16-18, Postbus 88, 1530 AB Wormer,
the Netherlands, ton.vanthoff@bruker.nl

Vrielinck Henk, Department of Solid State Sciences, UGent, Krijgslaan 281-S1, 9000 Gent,
henk.vrielinck@ugent.be

Yavkin Boris, Experimental condensed matter, University of Antwerp, Universiteitsplein 1,
2610 Wilrijk, boris.yavkin@gmail.com